

Functional Domains of the *Saccharomyces cerevisiae* Mlh1p and Pms1p DNA Mismatch Repair Proteins and Their Relevance to Human Hereditary Nonpolyposis Colorectal Cancer-Associated Mutations

QISHEN PANG,¹ TOMAS A. PROLLA,² AND R. MICHAEL LISKAY^{1*}

Department of Molecular and Medical Genetics, Oregon Health Sciences University, Portland, Oregon 97201-3098,¹ and Department of Molecular and Human Genetics, Baylor College of Medicine, Houston, Texas 77030²

Received 28 February 1997/Returned for modification 11 April 1997/Accepted 19 May 1997

The MutL protein is an essential component of the *Escherichia coli* methyl-directed mismatch repair system but has no known enzymatic function. In the yeast *Saccharomyces cerevisiae*, the MutL equivalent, an Mlh1p and Pms1p heterodimer, interacts with Msh2p bound to mismatch-containing DNA. Little is known of the functional domains of Mlh1p and Pms1p. In this report, we define the Mlh1p and Pms1p domains required for Mlh1p-Pms1p interaction. The Mlh1p-interactive domain of Pms1p is comprised of 260 amino acids near the carboxyl terminus while the Pms1p-interactive domain of Mlh1p resides in the final 212 residues. The two domains are sufficient for Mlh1p-Pms1p interaction, as determined by the two-hybrid assay and by *in vitro* protein affinity chromatography. Deletions within the domains completely eliminated Mlh1p-Pms1p interaction. Using site-directed mutagenesis, we altered a number of highly conserved residues in the Mlh1p and Pms1p proteins, including some alterations that mimic germline mutations observed for human hereditary nonpolyposis colorectal cancer. Alterations either in the consensus MutL box located in the amino-terminal portion of each protein or in the carboxyl-terminal homology motif of Mlh1p eliminated DNA mismatch repair function but had no effect on Mlh1p-Pms1p interaction. In addition, certain *MLH1* and *PMS1* mutant alleles caused a dominant negative mutator effect when overexpressed. We discuss the implications of these findings for the structural organization of the Mlh1p and Pms1p proteins and the importance of Mlh1p-Pms1p interaction.

In both prokaryotes and eukaryotes, DNA mismatch repair (DMR) plays several roles in DNA metabolism, including the repair of mispaired bases that result from DNA replication, repair of DNA mismatches that arise due to spontaneous deamination of 5-methylcytosine or chemical base damage, and repair of mispairs that form during genetic recombination (40). In humans, mutations in the DMR genes *MSH2*, *MLH1*, *PMS2*, and *PMS1* are associated with hereditary nonpolyposis colorectal cancer (HNPCC) (12, 18, 29, 43, 44, 55; reviewed in reference 26). Mutation of DMR genes has also been observed at a variable frequency in a number of sporadic tumors (26, 33, 52). In mice, disruptions of the mouse DMR genes *MSH2*, *PMS2*, and *MLH1* result in microsatellite instability and increased tumor development (6, 7, 14, 49). Additionally, *PMS2*- and *MLH1*-deficient mice display abnormalities in meiotic chromosome synapsis and reciprocal exchange, respectively (6, 7, 16).

Biochemical studies with *Escherichia coli* indicate that methyl-directed DMR is initiated through the action of three proteins, MutS, MutL, and MutH (39). The MutS protein recognizes DNA mismatches, and MutH is an endonuclease that directs repair to the newly synthesized strand (39). Although no biochemical activity of MutL has been demonstrated, the MutL protein appears to couple mismatch recognition by MutS to MutH activation in an ATP-dependent manner. Furthermore, DNase I protection experiments have shown that the MutL protein interacts with a MutS-heteroduplex DNA

complex in the presence of ATP (20). In the yeast *Saccharomyces cerevisiae*, DMR employs three MutS homologs, Msh2p, Msh3p, and Msh6p (10, 26, 36, 41), and two MutL homologs, Mlh1p and Pms1p (27, 28, 46). In both yeast and human, Msh2p appears to form heterodimers with either Msh3p or Msh6p, with the two heterodimer species displaying different DNA mismatch recognition specificities (1, 2, 15, 22, 23, 25, 36, 43). We have previously reported that Mlh1p and Pms1p form a heterodimer or higher-order multimer that binds to an Msh2p-heteroduplex DNA complex *in vitro* (47). *In vivo*, additional factors are likely to interact with Mlh1p and Pms1p during the DMR process. Recent studies have identified one such factor, the DNA replication processivity factor PCNA. Those studies suggested that PCNA interacts with human PMS2 (hPMS2) and, in the case of yeast, with both Mlh1p and Msh2p and that PCNA is required for an early step in mismatch repair (54). This interaction suggests a tight linkage between the DNA replication apparatus and DMR, possibly reflecting one aspect of the strand discrimination mechanism.

Despite our growing understanding of the role of DMR mutations in human and mouse tumorigenesis, little is known regarding the functional domains of DMR proteins. Previous work has shown that the bacterial MutS protein contains an ATP binding domain and that mutations in this domain alter both the ATPase and the mismatch binding activities of MutS (21, 57). Recent studies with yeast have shown that site-directed mutagenesis of the ATP binding domain of Msh2p did not affect initial mismatch recognition but caused a dominant negative effect when overexpressed in wild-type cells (4). A screen for dominant negative alleles of the bacterial mutL gene has identified several amino acid substitutions, mainly in the amino-terminal portion of the protein (5). In humans, specific

* Corresponding author. Mailing address: Department of Molecular and Medical Genetics, L103, Oregon Health Sciences University, Portland, OR 97201-3098. Phone: (503) 494-3475. Fax: (503) 494-6886. E-mail: liskaym@ohsu.edu.

mutations in two hMutL homologs, hMLH1 and hPMS2, apparently result in altered proteins that abolish DMR, possibly in a dominant negative manner, and lead to early tumor development (45). Here we report the use of site-directed mutagenesis and two-hybrid assays to determine functional domains in yeast Mlh1p and Pms1p that are critical for DMR, heterodimerization, and possibly interaction with other proteins. Additionally, our results provide a framework for understanding the consequences of specific DMR mutations observed in human cancer and provide rationales for identifying additional components in the process.

MATERIALS AND METHODS

Strains and growth conditions. *E. coli* DH1 was used for all plasmid constructions. Maltose binding protein (MBP) fusion proteins were expressed in *E. coli* PR78 (*lon::Tn10Δ16Δ17 argE(Am) Spe^r Rif^r araD139 galE galK phoAΔ20 thi*). The yeast two-hybrid reporter strain L40 of *S. cerevisiae* (56) was used for the in vivo interaction studies. For mutational analysis and overexpression of hemagglutinin 1 (HA1)-tagged proteins, the yeast strain MW3317-21A and its *mlh1Δ* and *pms1Δ* derivatives were used (46). Yeast cells were grown on YPD (1% Bacto yeast extract, 2% Bacto peptone, 2% glucose, 2% agar) or appropriate selective “dropout” medium (0.7% yeast nitrogen base, 0.5% ammonium sulfate, 2% glucose, 2% agar, and 0.09% dropout mix lacking the amino acid used for selection).

Plasmid constructions and site-directed mutagenesis. (i) Plasmid constructs. All DNA manipulations were carried out by using standard methods (34). Plasmids pGAD-yMLH1, pGAD-yPMS1, pBTM-yMLH1, and pBTM-yPMS1 were constructed by cloning the coding sequences for the yeast Mlh1p and Pms1p proteins into the two-hybrid vectors pGAD424 (8) and pBTM116 (56), respectively.

For constructing the yeast *MLH1* complementation plasmid pCOM-yMLH1, an *SphI-SmaI* fragment in yeast vector YCp50 containing the *URA3* gene was replaced with a *TRP1*-containing *SphI-PvuII* fragment from pBTM116. This created plasmid YCp-TRP1. Then an *SphI-PvuII* fragment containing the yeast *MLH1* gene from the original YEp24-yMLH1 plasmid (46) was inserted into the *SphI* and *EcoRI* (blunted) sites of YCp-TRP1. The resulting plasmid only partially complemented the *mlh1Δ* strain. Therefore, an *XbaI* (blunted)-*ClaI* fragment of the 5' *MLH1* sequence (46) was inserted into the partial-complementation plasmid, predigested with *NaeI* in YCp-TRP1 and *ClaI* in the *MLH1* gene, to create plasmid pCOM-yMLH1, which fully complements the *mlh1Δ* strain.

Plasmids pMAL-yMLH1 and pMAL-yPMS1 have been previously described (47). The pMAL constructs expressing residues 1 to 265 of Mlh1p [Mlh1p(1–265)], Mlh1p(501–769), Pms1p(1–271), and Pms1p(692–904) were prepared by subcloning the corresponding cDNA fragments (see “Deletion mutants” below) into the multiple-cloning site of the pMAL vector.

MLH1 and *PMS1* constructs, used to test for dominant negative effect and protein stability, were created in pCoB-5006 and pJAS. pCoB-5006 was constructed as follows. A 405-bp *SphI* (blunted)-*HindIII* fragment containing the alcohol dehydrogenase I (ADH) gene promoter and a 230-bp *EcoRI-SphI* (blunted) fragment containing the ADH gene terminator from pBTM116 were inserted into pBluescript II SK⁻ (Stratagene) at the *HincII-HindIII* and *EcoRI-SphI* (blunted) sites, respectively, to create pADH. This ADH promoter/terminator cassette was used to replace the fragment containing the ADH promoter-*lexA*-ADH terminator sequence in pBTM116 by digesting pADH with *Bss*HIII and pBTM116 with *SphI* and end filling both the pBTM116 vector and the ADH promoter/terminator cassette with T4 DNA polymerase. pJAS was created by PCR amplifying the ADH promoter sequence from yeast genomic DNA and replacing the 420-bp *XhoI-EcoRI* ADH promoter fragment in pCoB-5006 with the PCR fragment. This step created an *NcoI* site and an ATG start codon at the 3' end of the ADH promoter. *Bam*HI-*Sall* fragments encoding full-length (wild type or with point mutations) and amino-terminal portions (see “Deletion mutants” below) of Mlh1p or Pms1p were cloned into the corresponding sites of pCoB-5006. For carboxyl-terminal Mlh1p and Pms1p constructs, the truncated Mlh1p- and Pms1p-encoding fragments were fused in frame with the ATG start codon in pJAS.

Epitope-tagged constructs were made by insertion of triple tandem HA1 epitope sequences as described previously (50). Briefly, PCR primers were used to introduce a *NotI* site immediately upstream of the termination codon of full-length or truncated *MLH1* or *PMS1* (in the pCoB vector) and a *Sall* site at the end of the HA1 triple peptides (53). Then, a *NotI-Sall* fragment containing the HA1 triple tag was cloned into the corresponding site of the modified *MLH1* or *PMS1* plasmid.

(ii) Deletion mutants. Deletion derivatives of *MLH1* were generated by using the following naturally occurring restriction sites: *Bgl*II at position 2279–2284 [Mlh1p(1–761)], *Xmn*I at position 2193–2202 [Mlh1p(1–731)], *Sca*I at position 1885–1890 [Mlh1p(1–629)], *Bsu*36I at position 1506–1512 [Mlh1p(1–502)] and Mlh1p(501–769), *Spe*I at positions 794–799 [Mlh1p(1–265)] and 1193–1198 [Mlh1p(397–769)], *Nde*I at position 376–381 [Mlh1p(1–126)], and *Hind*III at

position 1665–1670 [Mlh1p(555–769)]. For the Pms1p deletions, the internal restriction sites used to generate the truncated proteins were as follows: *Nco*I at position 2649–2654 [Pms1p(1–881)], *Hpa*I at position 2091–2096 [Pms1p(1–693) and Pms1p(692–904)], *Spe*I at position 1588–1593 [Pms1p(1–525) and Pms1p(524–904)], *Bsm*I at position 827–833 [Pms1p(1–271)], and *Sph*I at position 2208–2213 [Pms1p(735–904)]. A stop codon was generated at the 3' deletion endpoint of each Mlh1p and Pms1p derivative by fusion to a linker, AGGCCCTAATTAATTAATTAATTAATTAAGTCGAC. For making Pms1p(1–152), the K153 codon AAG was changed to TAG by PCR-mediated mutagenesis (37).

(iii) Point mutations. All amino acid substitutions in the Mlh1p protein were introduced by PCR mutagenesis (37) with oligonucleotides encoding the following mutations. For changing alanine (A) to phenylalanine (F), glycine (G), or serine (S) at position 41, the forward primer, encoding amino acid residues 36 to 45 of MLH1, was used to modify the protein at position 41 to phenylalanine, glycine, or serine. The 268-bp PCR-generated fragments encoding the A-to-F, A-to-G, and A-to-S substitutions were used to replace the corresponding fragments in pCOM-yMLH1 and pGAD-yMLH1 to create the mutants A41F, A41G, and A41S, respectively.

To mutagenize the MutL box GFRGEAL of the Mlh1p protein, the *Bam*HI-*AccI* fragment from pGAD-yMLH1 was subcloned into pBluescript SK⁻ (Stratagene) to create pYMLH1-BA. The sequence corresponding to residues 37 to 100 of Mlh1p with *Cla*I and *Hind*III restriction sites at the 5' and 3' ends, respectively, was amplified by PCR. The reverse primer encoding amino acid residues 94 to 102 of Mlh1p, having a new codon in place of the codon for phenylalanine, arginine (R), or glycine, was used to modify the protein at position 96, 97, or 98, respectively, to alanine or valine (V). The 187-bp PCR products digested with *Cla*I and *Hind*III were ligated into *Cla*I- and *Hind*III-digested pYMLH1-BA. Then the *Bam*HI-*Nde*I or *Cla*I-*Nde*I fragment from the resulting plasmids was used to replace the corresponding fragment in pGAD-yMLH1 or pCOM-yMLH1 to create the mutants F96A, R97A, G98A, and G98V. To create the Pms1p MutL box mutant Pms1p-F126A, recombinant PCR (34) was used to modify the *PMS1* gene in pGAD-yPMS1. Primers in both the 5'-to-3' and the 3'-to-5' directions, encoding amino acid residues 122 to 130, were used to change the phenylalanine residue at position 126 to alanine. The same technique was employed to create Mlh1p-K619del, produced by an in-frame deletion of codon K619. In this case, primers in both the 5'-to-3' and the 3'-to-5' directions, encoding amino acid residues 614 to 624, were used to delete codon K619.

The point mutation constructs encoding the carboxyl-terminal homology (CTH) motif (final 13 amino acids) of Mlh1p were created in pMAL-yMLH1. Briefly, a 524-bp sequence, which encompassed codons for the final 10 amino acids of Mlh1p and the conjunctive 3' untranslated region, was PCR amplified by using a forward primer that included a single point mutation and a *Bgl*II site and by using a reverse primer with another *Bgl*II site. This PCR product was inserted into the *Bgl*II site in pMAL-yMLH1. *Bsu*36I-*Sall* and *Cla*I-*Sall* fragments from pMAL-yMLH1, each encoding a K764-to-E or -R, F766-to-A, E767-to-D, or C769-to-A or -S substitution, were used to replace the corresponding fragments in pGAD-yMLH1 and pCOM-yMLH1, respectively, to create the mutants K764E, K764R, F766A, E767D, C769A, and C769S. All mutation-containing alleles were subjected to sequence analysis to confirm that the desired changes had occurred.

Yeast transformation and β-galactosidase assays. Yeast transformation was performed by the polyethylene glycol-lithium acetate method (19). For the color filter assay, colonies with pairing hybrids were lifted on nitrocellulose filters (Schleicher and Schuell BA-S85), frozen in liquid nitrogen, and incubated at 30°C on filter paper soaked with Z buffer (38). To measure β-galactosidase activity, cells were resuspended in 0.5 ml of Z buffer with 0.64 mg of *o*-nitrophenyl-β-D-galactosidase substrate per ml and permeabilized with chloroform. Reactions were stopped with Na₂CO₃ when an appropriate level of color had developed. β-Galactosidase activity was calculated by the equation: U/h = [(OD₄₂₀/OD₆₀₀) · 60]/min, where OD₄₂₀ and OD₆₀₀ are the optical densities at 420 and 600 nm.

Measurement of mutation rates. To measure the reversion rates of the *hom3-10* allele, wild-type MW3317-21A and its *mlh1Δ* and *pms1Δ* derivatives with various complementation plasmid constructs were grown to saturation in minimal medium lacking tryptophan. Cells were then plated on selective medium lacking both tryptophan and threonine. Colonies appearing after 3 days of growth at 30°C were counted. The rate of *hom3-10* reversion was determined by fluctuation analysis as previously described (3, 32, 46). For each mutation rate, 12 independent cultures were tested.

In vitro protein interactions. The expression and purification of the MBP fusion proteins were performed as recommended by the manufacturer (New England BioLabs). Protein concentrations were determined by Bradford analysis (11) with bovine serum albumin as a standard. [³⁵S]methionine-labeled proteins were prepared by in vitro transcription and translation, using the rabbit reticulocyte lysate system (Novagen). Twenty microliters of [³⁵S]methionine-labeled proteins were added to MBP fusion protein columns. After washing with 10 volumes of buffer (20 mM Tris-HCl [pH 7.4], 200 mM NaCl, 1 mM EDTA), the bound proteins were eluted in the same buffer containing 10 mM maltose and examined by sodium dodecyl sulfate-polyacrylamide gel electrophoresis (SDS-PAGE) followed by autoradiography.

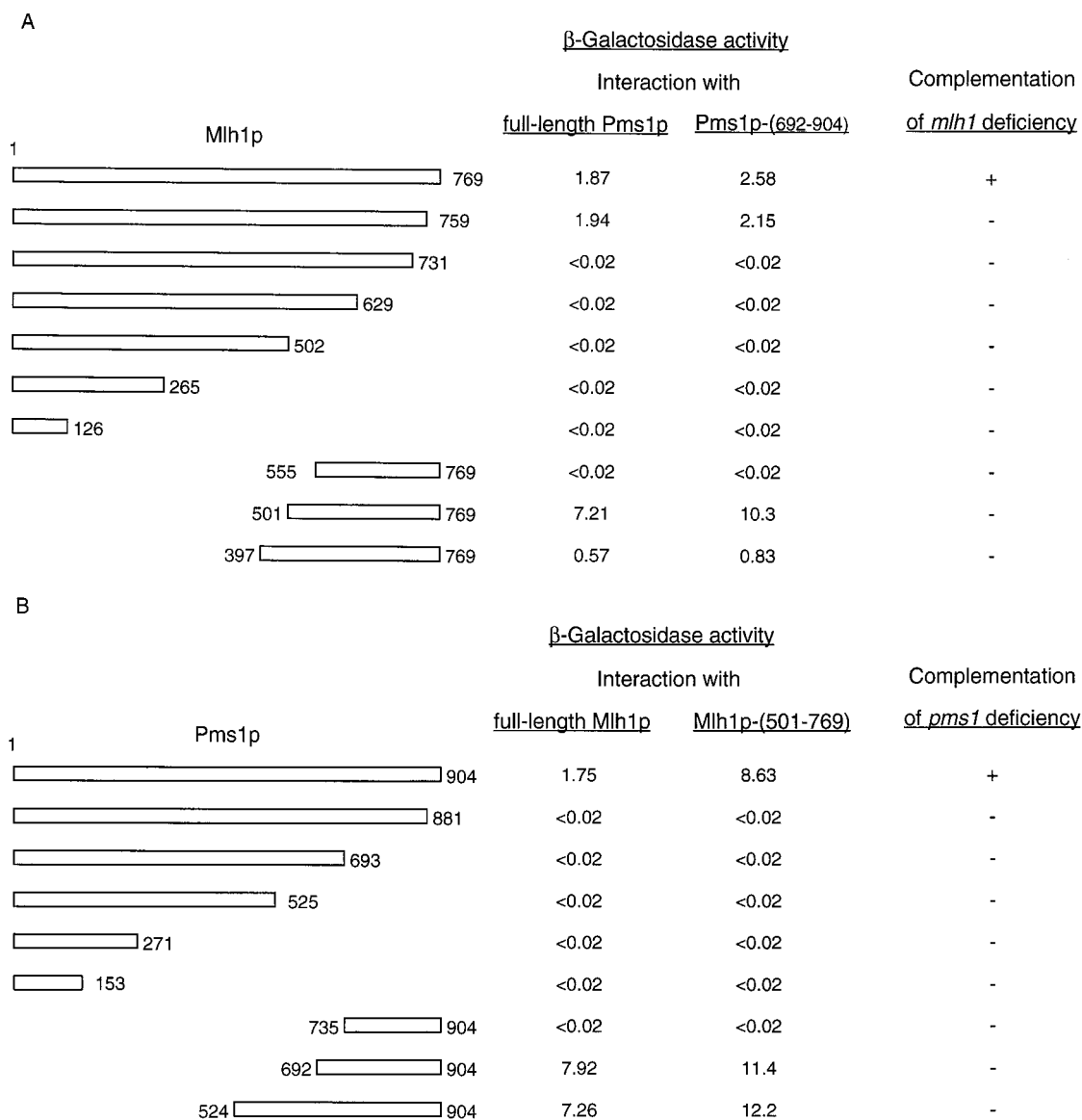


FIG. 1. Mapping of the interactive domains in Mlh1p and Pms1p. (A) Full-length (residues 1 to 769) or truncated Mlh1p was fused to the GAL4 activation domain, and the hybrid proteins were assayed in *S. cerevisiae* L40 for the ability to interact with either full-length Pms1p or the Mlh1p-interactive domain of Pms1p [Pms1p (692-904)] fused to the LexA DNA binding domain. The relevant Mlh1p sequences are illustrated diagrammatically, with the amino acid residues of Mlh1p contained in each construct represented by the rectangles. Interaction was quantitated by β -galactosidase assays as described in Materials and Methods, and the values shown represent averages of the units of β -galactosidase activity from three independent assays. The variation in the relative β -galactosidase activities was within 10%. Complementation of *mlh1* deficiency was determined by a replica-plating analysis of the *hom3-10* reversion. For each construct, four patches were grown on selective medium in a 100- by 15-mm petri dish. +, 0 to 1 colonies of *hom3-10* revertants per patch; -, 30 to 50 colonies of *hom3-10* revertants per patch. (B) Schematic illustration of PMS1 derivatives fused to the GAL4 activation domain and their interaction with either full-length Mlh1p or the Pms1p-interactive domain of Mlh1p [Mlh1p(501-769)] fused to the LexA DNA binding domain. β -Galactosidase levels and complementation of *pms1* deficiency were determined as described for panel A; +, 0 to 1 colonies of *hom3-10* revertants, -, 30 to 50 colonies of *hom3-10* revertants.

Immunoblot analysis. The relative stabilities of the mutant Mlh1p and Pms1p proteins were assessed by Western blotting of yeast extracts. Cells with constructs encoding full-length Mlh1p and Pms1p and the truncated mutants Mlh1p(1-265) and Pms1p(1-271) were grown in 10 ml of minimal medium lacking tryptophan to a density of 2×10^7 cells/ml. Only these two truncated mutants were assayed for stability, because they demonstrated a different dominant negative effect in wild-type cells. Cells were pelleted, resuspended in 10 volumes of sample buffer (60 mM Tris [pH 6.8], 2% SDS, 100 mM dithiothreitol, 10% glycerol, 0.01% bromophenol blue), and broken by vortexing with an equal volume of glass beads (eight 15-s bursts). The lysate was boiled for 5 min, cleared by sonication for 15 s to shear DNA, and spun for 10 min at 12,000 rpm in a microcentrifuge. Ten microliters of this lysate was electrophoresed on a standard SDS-8% polyacrylamide gel and blotted to a nitrocellulose filter. The blot was preincubated in 6% nonfat dried milk prepared in TBS (20 mM Tris-HCl [pH 7.6] and 150 mM

NaCl) and probed with a 1:400 dilution of monoclonal antibody 12CA5 (Boehringer Mannheim). The secondary antibody was a goat anti-mouse horseradish peroxidase-conjugated immunoglobulin G antibody used at a 1:5,000 dilution (Pierce, Rockford, Ill.). The blot was visualized with chemiluminescent reagents from National Diagnostics (Atlanta, Ga.).

RESULTS

Identification of domains in Mlh1p and Pms1p sufficient for Mlh1p-Pms1p interaction. Evidence from yeast and human cells suggests that Mlh1p (hMLH1) and Pms1p (hPMS2) are likely to function as a heterodimer (30, 47). To investigate the

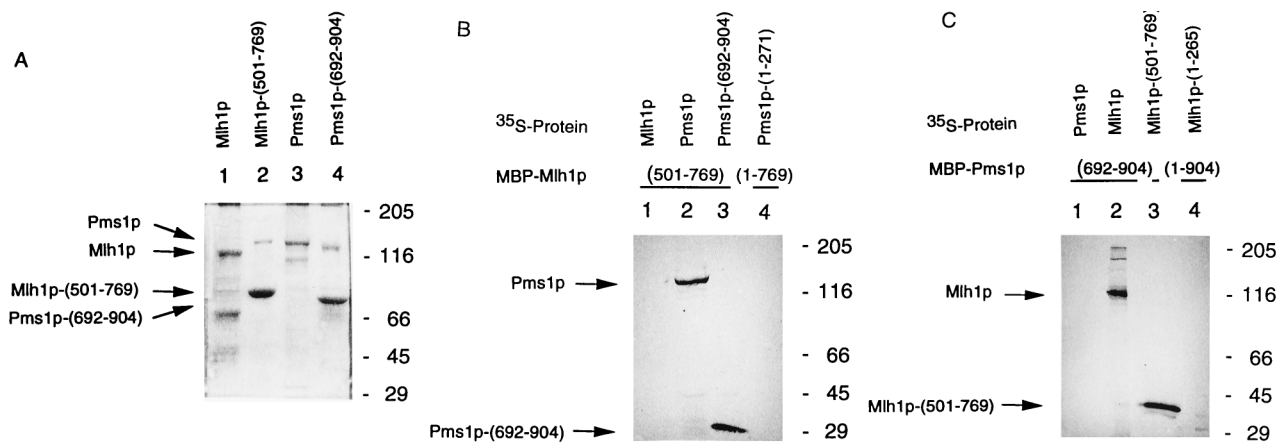


FIG. 2. Association between the interactive domains of Mlh1p and Pms1p in vitro. (A) MBP fusion proteins were prepared with amylose affinity columns as described in Materials and Methods, separated by SDS-PAGE (8% polyacrylamide), and stained with Coomassie blue. Lane 1, MBP-Mlh1p; lane 2, MBP-Mlh1p(501–769); lane 3, MBP-Pms1p; lane 4, MBP-Pms1p(692–904). Molecular size markers (in kDa) migrated as indicated. (B) Interaction of Mlh1p(501–769) with [³⁵S]methionine-labeled proteins. MBP fusion proteins were loaded onto amylose columns with [³⁵S]methionine-labeled proteins. Eluted proteins from these columns were resolved by SDS-PAGE (8% polyacrylamide) and analyzed by autoradiography. Lane 1, MBP-Mlh1p(501–769) plus [³⁵S]methionine-labeled full-length Mlh1p; lane 2, MBP-Mlh1p(501–769) plus [³⁵S]methionine-labeled full-length Pms1p; lane 3, MBP-Mlh1p(501–769) plus [³⁵S]methionine-labeled Pms1p(692–904); lane 4, MBP-Mlh1p plus [³⁵S]methionine-labeled Pms1p(1–271). (C) Interaction of Pms1p(692–904) with [³⁵S]methionine-labeled proteins. Lane 1, MBP-Pms1p(692–904) plus [³⁵S]methionine-labeled full-length Pms1p; lane 2, MBP-Pms1p(692–904) plus [³⁵S]methionine-labeled full-length Mlh1p; lane 3, MBP-Pms1p(692–904) plus [³⁵S]methionine-labeled Mlh1p(501–769); lane 4, MBP-Pms1p plus [³⁵S]methionine-labeled Mlh1p(1–265).

domains responsible for Mlh1p-Pms1p interaction, we constructed a series of yeast Mlh1p and Pms1p deletion mutants and tested the truncated proteins for interaction by using the yeast two-hybrid system. As shown in Fig. 1A, all but one carboxyl-terminal truncation of Mlh1p failed to interact with Pms1p. A carboxyl-terminal portion of Mlh1p corresponding to residues 501 to 769, Mlh1p(501–769), interacted with Pms1p, whereas Mlh1p(555–769) failed to bind to full-length Pms1p, suggesting that the Pms1p-interactive domain of Mlh1p lies in the carboxyl portion of Mlh1p. Interestingly, even though the final 13 amino acids are identical in the yeast and human MLH1 homologs (12, 44), this CTH motif of yeast Mlh1p apparently is not required for Pms1p interaction because deletion of the final eight amino acids of Mlh1p did not affect Mlh1p-Pms1p interaction as assayed in the two-hybrid system. We observed a reduced interaction of Mlh1p(397–769) with Pms1p, compared with the interactions observed for Mlh1p(501–769) and full-length Mlh1p. This weaker signal could be due to a reduced interaction or to either protein instability or abnormal folding. All *mlh1* deletion mutants showed a strong mutator phenotype as determined by a replica-plating assay of the *hom3-10* reversion (Fig. 1A).

Among Pms1p truncations (Fig. 1B), two carboxyl-terminal fragments, PMS1(692–904) and PMS1(524–904), showed strong interactions with full-length Mlh1p. In contrast, Pms1p(735–904) showed no interaction with Mlh1p. Again, by using the *hom3-10* reversion assay, each of the *pms1* deletion mutants were nonfunctional in repair. Further analysis showed that Mlh1p(501–769) interacted strongly with Pms1p(692–904) (see the third columns in Fig. 1A and B). The 10-fold higher apparent interaction relative to that observed for the full-length parent pair may result from an actual stronger interaction or from higher expression and/or increased stability of the truncated products. Taken together, the results of these two-hybrid assays suggest that domains within residues 501 to 769 of Mlh1p and residues 692 to 904 of Pms1p are primarily involved in Mlh1p-Pms1p interaction.

In vitro studies of the interactive domains. As a second means to define the domains sufficient for Mlh1p-Pms1p in-

teraction, we tested the ability of Mlh1p(501–769) and Pms1p(692–904), expressed as stable fusion proteins with MBP in *E. coli* (Fig. 2A), to bind a series of [³⁵S]methionine-labeled proteins in a protein affinity chromatography assay. As indicated in Fig. 2B, [³⁵S]methionine-labeled full-length Pms1p and Pms1p(692–904) were retained specifically on the MBP-Mlh1p(501–769) column (lanes 2 and 3). Full-length Mlh1p did not interact with the Pms1p-interactive domain, Mlh1p(501–769) (lane 1), consistent with our previous observations (47). The amino-terminal Pms1p(1–271) (lane 4) showed no interaction with Mlh1p. As previously demonstrated (47), both full-length Pms1p and Pms1p(692–904) bound to a column containing full-length Mlh1p (data not shown).

The column with MBP-Pms1p(692–904) retained [³⁵S]methionine-labeled full-length Mlh1p and Mlh1p(501–769) (Fig. 2C, lanes 2 and 3) but not full-length Pms1p (lane 1). Consistent with the two-hybrid results, the full-length Pms1p column did not retain the amino-terminal Mlh1p(1–265) (lane 4). In a separate experiment, a full-length Pms1p column retained both full-length Mlh1p and Mlh1p(501–769) (data not shown). Neither Mlh1p(501–769) nor Pms1p(692–904) bound to a control column with MBP only (data not shown). These results are consistent with the two-hybrid studies presented above and strongly suggest that residues 501 to 769 of Mlh1p and residues 692 to 904 of Pms1p represent the primary domains necessary for Mlh1p-Pms1p interaction.

The effects of mutations in the MLH domain on mismatch repair function and Mlh1p-Pms1p interaction. Most known MutL homologs, including yeast Mlh1p and Pms1p, have significant homology (approximately 50% identical) in a stretch of 90 amino acids in the amino terminus (12, 44, 46) (Fig. 3A). The region, which we refer to as the MutL homology (MLH) domain, encompasses the MutL box sequence GFRGEAL, which is identical in most MutL homologs (Fig. 3A). To examine the structural and functional properties of the MLH domain, we made alanine substitutions at amino acid positions F96, R97, and G98 in the MutL box of yeast Mlh1p. This alanine mutagenesis strategy presumes that, while the functional group of the natural amino acid is removed, the alanine

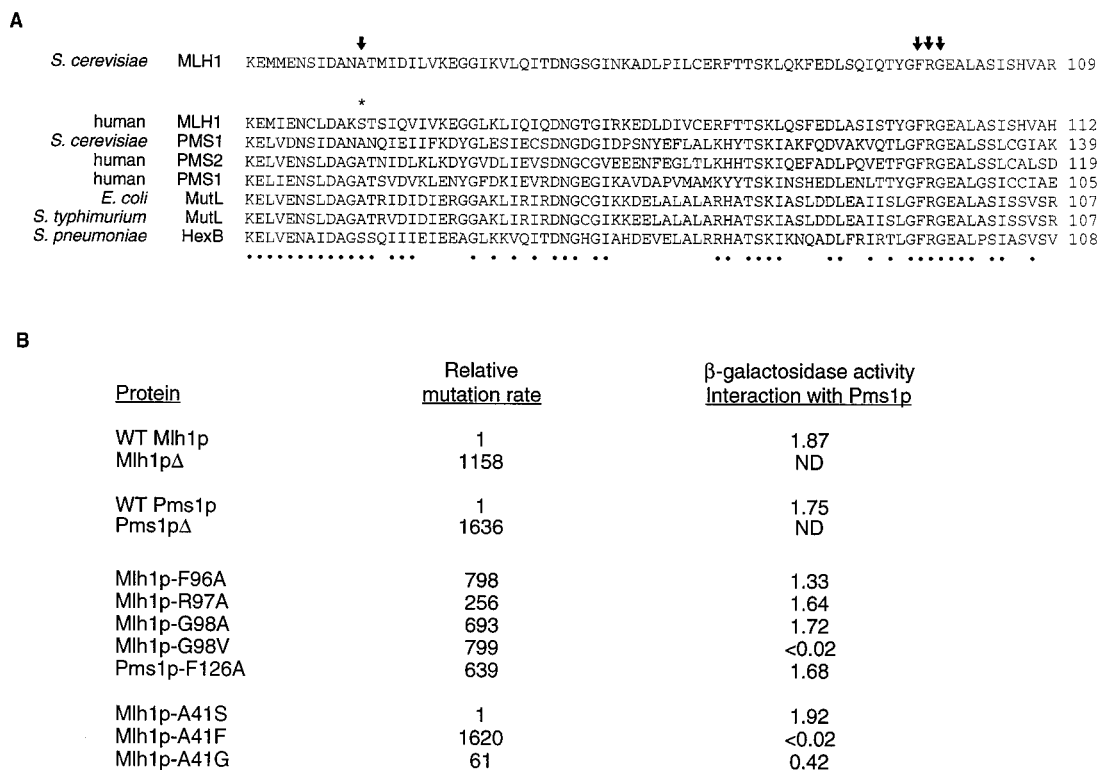


FIG. 3. Effects of mutations in the MLH domain on DMR function and Mlh1p-Pms1p interaction. (A) Sequence comparisons of the MLH domains of the MutL homologs *S. cerevisiae* Mlh1p (46), hMLH1 (12), *S. cerevisiae* Pms1p (27), hPMS2 (42), human PMS1 (42), *E. coli* MutL (31), *Salmonella typhimurium* MutL (35), and *Streptococcus pneumoniae* HexB (48). Amino acids that are identical for at least five proteins are marked with a dot. The arrowheads indicate the positions at which amino acid changes were made. The asterisk denotes the predicted amino acid change S44F in the hMLH1 HNPCC mutation (12). (B) DMR function and interaction of wild-type (WT) and mutant proteins. Mutation rates were determined by the fluctuation assay as described in Materials and Methods and are presented relative to the rate observed for WT Mlh1p (9.5×10^{-9}) or WT Pms1p (1.1×10^{-8}). The strains used to determine the null mutation rates of Mlh1Δ and Pms1pΔ have been described previously (46). ND, not determined. Interaction was quantitated as described in the legend to Fig. 1.

substitutions do not perturb the overall structure or stability of the protein (13). As shown in Fig. 3B, alanine substitutions at F96, R97, and G98 resulted in loss of mismatch repair function as determined by the inability to complement a yeast *mlh1Δ* mutation but did not affect interaction with Pms1p. However, substitution of glycine at residue 98 with the larger and more hydrophobic valine not only caused a strong mutator phenotype but also abolished binding to Pms1p. We also demonstrated that a Pms1p mutant with a point mutation in the MutL box, Pms1p-F126A (analogous to Mlh1p-F96A), also showed a strong mutator phenotype but retained interaction with Mlh1p.

Previous studies showed that an S44F substitution in the MLH domain of hMLH1 was a likely cause of HNPCC (12). To test the effect of an analogous mutation in yeast, we introduced point mutations at position A41 of yeast Mlh1p. At position 41, yeast Mlh1p contains alanine whereas hMLH1 contains serine (12) (Fig. 3A). As shown in Fig. 3B, the replacement of the alanine with serine in yeast Mlh1p did not affect either repair function or Mlh1p-Pms1p interaction. In contrast, substitution with phenylalanine at position 41 in yeast Mlh1p resulted in loss of both mismatch repair function, equivalent to a null mutation, and interaction with Pms1p. Interestingly, the replacement of A41 with a structurally similar glycine had only a minor effect on both repair function and binding of Pms1p. These results support the finding that the hMLH1 mutation S44F is causal in HNPCC families carrying this mutation (see Discussion).

Mutations in the CTH motif of Mlh1p cause loss of DMR function but do not affect interaction with Pms1p. The final 13 amino acids of the yeast Mlh1p and the hMLH1 proteins are identical (12, 44) (Fig. 4A). The deletion studies described above suggest that this portion of yeast Mlh1p is not involved in Mlh1p-Pms1p interaction (Fig. 1A). However, this highly conserved motif is required for mismatch repair function because deletion of the final eight amino acids [Mlh1p(1-761)] resulted in a strong mutator phenotype (Fig. 1A). To identify important residues responsible for mismatch repair function, we generated missense mutations in the CTH motif of the yeast Mlh1p protein. These missense mutations were tested for complementation of a yeast *mlh1Δ* strain and interaction with Pms1p. As shown (Fig. 4B), these substitutions had no effect on interaction with Pms1p, consistent with our deletion analysis (Fig. 1A). By contrast, most substitutions at positions K764, F766, E767, and C769 resulted in repair-deficient alleles. While the conservative substitution K764R retained mismatch repair activity, K764E and F766A eliminated function. Surprisingly, the conservative change E767D resulted in loss of mismatch repair function. Possibly, E767 is involved in amino acid-amino acid contact that the slightly smaller aspartic acid cannot accommodate. These results further confirm that the CTH motif of Mlh1p is essential for DMR but not for Mlh1p-Pms1p interaction and indicate that Mlh1p-Pms1p interaction is necessary but not sufficient for mismatch repair function.

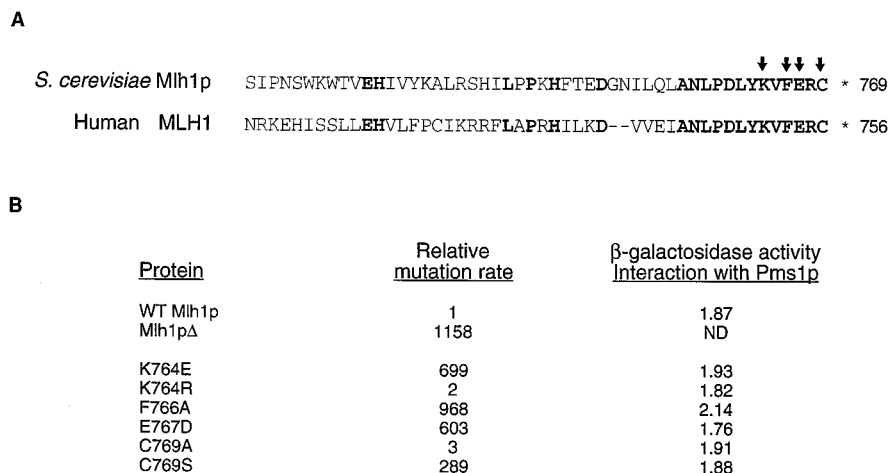


FIG. 4. The CTH motif of Mlh1p is necessary for DMR function but not Mlh1p-Pms1p interaction. (A) An alignment between the carboxyl-terminal parts of the yeast Mlh1 and the hMLH1 proteins. Identical amino acids are shown in boldface. The arrowheads indicate the positions at which amino acid changes were made. Asterisks denote the end of each protein. (B) DMR function and interaction of wild-type and mutant proteins. Mutation rates were determined by the fluctuation assay as described in Materials and Methods and are presented relative to the rate observed for the wild-type (WT) Mlh1p, which is 9.5×10^{-9} . The strain used to determine the null mutation rate of Mlh1pΔ has been described previously (46). ND, not determined. Interaction was quantitated as described in the legend to Fig. 1.

Certain MLH1 and PMS1 mutations show dominant negative effects. As described above, mutational analysis of the yeast Mlh1p and Pms1p proteins revealed two elements of unknown function, the MutL box and the CTH motif, both of which are required for DMR but are apparently not involved in Mlh1p-Pms1p complex formation. The presence of excess protein altered in these functional domains could block DMR in a wild-type cell due to either the formation of a nonfunctional repair complex or the inability to interact with other components. We overexpressed several altered Mlh1p proteins, constructed in a yeast expression vector under an ADH promoter, in a wild-type strain and tested for mutator activity. Altered Mlh1p and Pms1p constructs containing the Pms1p-interaction domain of Mlh1p [Mlh1p(501–769)] and the Mlh1p-interaction domain of Pms1p [Pms1p(692–904)] caused mutator phenotypes in wild-type cells (Table 1). Construct Mlh1p(1–761), which was deleted for the CTH motif, and the MutL box mutants Mlh1p-F96A and Pms1p-F126A also exhibited a dominant negative mutator effect in wild-type cells.

We also overexpressed Mlh1p and Pms1p sequences that do not show interaction with full-length Pms1p and Mlh1p. Overexpression of Mlh1p(1–265) and Mlh1p(734–769) exerted a dominant negative effect on mismatch repair (Table 1). Interestingly, Mlh1p-K619del overexpression, the equivalent of an HNPCC mutation associated with DMR deficiency in phenotypically normal human cells, also resulted in a dominant negative effect. The dominant negative effects resulting from Mlh1p(1–265), Mlh1p(734–769), and Mlh1p-K619del overexpression are apparently not mediated by interaction with PMS1.

In contrast to the effect observed with Mlh1p(1–265), overexpression of the Pms1p(1–271) fragment did not result in a dominant negative mutator effect. To determine whether this might be due to inappropriate expression or reduced stability of the Pms1p construct, full-length Mlh1p and Pms1p and the carboxyl-terminal truncations Mlh1p(1–265) and Pms1p(1–271) were tagged with an epitope corresponding to a nine amino-acid region of the HA protein of influenza virus (17). The tagged proteins were overexpressed in the wild-type cell and probed with a monoclonal HA antibody to determine the relative levels of the proteins. As indicated in Fig. 5, both Mlh1p(1–265) (lane 3) and Pms1p(1–271) (lane 5) were ex-

pressed at higher levels than full-length Mlh1p (lane 2) and Pms1p (lane 4). An additional lower band was observed in the Pms1p(1–271) sample, suggesting that the truncated protein was unstable in the cell. Thus, the relative instability of Pms1p(1–271) may account for the lack of a dominant negative effect.

DISCUSSION

Although the MutL protein is an essential component of the methyl-directed mismatch repair system in *E. coli*, little is known about MutL function. No enzymatic function or DNA mismatch specific binding activity has been reported for MutL. It has been proposed that MutL functions as a “molecular matchmaker,” presumably acting to stabilize the MutS-mismatch-DNA complex (51). Our previous studies suggested that in the yeast *S. cerevisiae* the MutL equivalent, a Mlh1p-Pms1p

TABLE 1. Dominant negative effects of certain Mlh1p and Pms1p constructs^a

Construct	Mutation rate in WT cells ^b	Interaction with Pms1p or Mlh1p ^c
Vector only	1.39×10^{-8} (1)	–
WT Mlh1p	7.66×10^{-9} (0.6)	+
WT Pms1p	1.06×10^{-8} (0.8)	+
Mlh1p(501–769)	2.12×10^{-6} (152)	+
Pms1p(692–904)	1.86×10^{-6} (134)	+
Mlh1p-K619del	6.19×10^{-7} (44.5)	–
Mlh1p(1–265)	3.98×10^{-7} (28.6)	–
Pms1p(1–271)	9.95×10^{-9} (0.7)	–
Mlh1p-F96A	7.85×10^{-6} (565)	+
Pms1p-F126A	3.57×10^{-6} (256)	+
Mlh1p(1–761)	3.33×10^{-6} (240)	+
Mlh1p(734–769)	4.56×10^{-7} (32.8)	–

^a Full-length or amino-terminal portions of the *MLH1* and *PMS1* cDNA sequences were subcloned in pCoB-5006; fragments encoding the carboxyl-terminal portions of both proteins were fused in frame with the ATG start codon in pJAS (see Materials and Methods). WT, wild type.

^b The mutation rate relative to that of the vector-only construct is shown in parentheses.

^c Interaction was determined by the two-hybrid assay; + and – indicate interaction and no interaction, respectively.

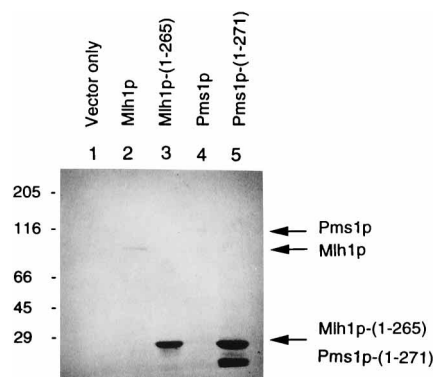


FIG. 5. Western blot analysis of HA-tagged proteins. Cell lysates were prepared from yeast cells containing full-length or truncated proteins tagged with an HA epitope and immunoblotted with monoclonal antibody 12CA5 as described in Materials and Methods. Lane 1, pCoB-5006 vector only; lane 2, full-length Mlh1p; lane 3, Mlh1p(1–265); lane 4, full-length Pms1p; lane 5, Pms1p(1–271). Note that lane 5 shows two products: the upper band corresponds to the expected Pms1p(1–271), and the lower band corresponds to a further truncated product. Molecular size markers (in kDa) migrated as indicated.

heterodimer, interacts with Msh2p bound to mismatch-containing DNA (47). In humans, MLH1 and PMS2 can be copurified as a heterodimer that complements the DMR defect in nuclear extracts of the colorectal tumor cell line defective in MLH1 (30). Through the use of the yeast two-hybrid system and of *in vitro* affinity protein chromatography, we have identified domains that appear to be primarily responsible for mediating the interaction between the yeast DMR proteins Mlh1p and Pms1p. Residues 501 to 769 of Mlh1p and residues 692 to 904 of Pms1p were shown to be required for Mlh1p-Pms1p interaction. *MLH1* and *PMS1* mutants in which these domains have been deleted failed to interact and were unable to complement *mlh1*- or *pms1*-deficient cells. Additionally, using site-directed mutagenesis, we have identified two highly conserved regions, namely the MutL box of both proteins and the CTH motif of Mlh1p, which are each necessary for DMR function but which are not required for Mlh1p-Pms1p interaction. We have also shown that certain Mlh1p and Pms1p mutants, with or without the interactive domains, exhibited dominant negative effects when overexpressed in wild-type cells.

The functional domains of the Mlh1p and Pms1p proteins as defined in this report are summarized in Fig. 6. Our results indicate that the carboxyl-terminal 33% of Mlh1p (not including the last 13 amino acids) and the carboxyl-terminal 23% of Pms1p are sufficient for Mlh1p-Pms1p interaction. Deletion of the interactive domains resulted in loss of both DMR function and Mlh1p-Pms1p interaction. However, deletion constructs containing only the Pms1p-interactive domain [Mlh1p(501–769)] or the Mlh1p-interactive domain [Pms1p(692–904)] retained Mlh1p-Pms1p dimerization activity but abolished DMR function. Therefore, Mlh1p-Pms1p interaction is necessary but not sufficient for DMR. There is no amino acid sequence homology between the two interactive domains of Mlh1p and Pms1p. However, the interacting regions of yeast Mlh1p and Pms1p have homology with the corresponding regions of their human counterparts, MLH1 and PMS2. We suggest that these homologous regions are responsible for interactions of the human proteins. In addition, during a two-hybrid search for Mlh1p-interacting proteins, we detected a protein with strong homology to Pms1p (51a). The carboxyl-terminal portion of this protein, which we refer to as Mlh3p, shows striking similarity to the final 200 amino acids of Pms1 corresponding to the

Mlh1p-interactive domain [Pms1p(692–904)]. These similarities are restricted to three subdomains with 25, 10, and 11 residues separated by about 100 and 20 residues, respectively (Fig. 7). Because these conserved subdomains are likely to comprise the elements necessary for binding of Pms1p and Mlh3p to Mlh1p, further study of these subdomains should be informative.

Results of two-hybrid assays and *in vitro* protein affinity chromatography indicate that Mlh1p-Pms1p interaction does not require amino-terminal portions of either protein. Our results do not exclude the possibility that the amino-terminal regions of Mlh1p and Pms1p play a role in maintaining a proper protein conformation necessary for the interaction. Two mutants with point mutations in the MLH domain of Mlh1p, Mlh1p-A41F and Mlh1p-G98V, disrupt Mlh1p-Pms1p interaction (Fig. 3B). Previously, it was suggested that alteration of hMLH1 by an S44F substitution, observed as the result of a germline mutation in an HNPCC family, was predicted to alter the hMLH1 protein conformation (12). Residue A41 of yeast Mlh1p, analogous to residue S44 of hMLH1, is in a highly conserved region of the MutL homologs (Fig. 3A). Chou-Fasman predictions suggest that both A41F and G98V substitutions change the predicted secondary structure in these regions and could therefore affect the overall conformation of Mlh1p. Alternatively, some regions in the amino-terminal domains of Mlh1p and Pms1p may have a role in heterodimer stabilization between full-length proteins *in vivo*.

An important implication of this study is that the highly conserved MLH domain of both proteins and the CTH motif of Mlh1p do not appear to be essential for Mlh1p-Pms1p interaction but are critical for DMR function. Figure 6 shows the region of highest conservation between Mlh1p and Pms1p, the MLH domain which encompasses the consensus MutL box sequence GFRGEAL, and a region with the final 13 amino acids identical between the yeast Mlh1p and the hMLH1 proteins (CTH motif). Most alterations in the MutL box and the CTH motif eliminated DMR function but not Mlh1p-Pms1p interaction, suggesting that these two functional domains have an intrinsic DMR activity and/or mediate interactions with other proteins in the DMR pathway. Relevant to the possibility

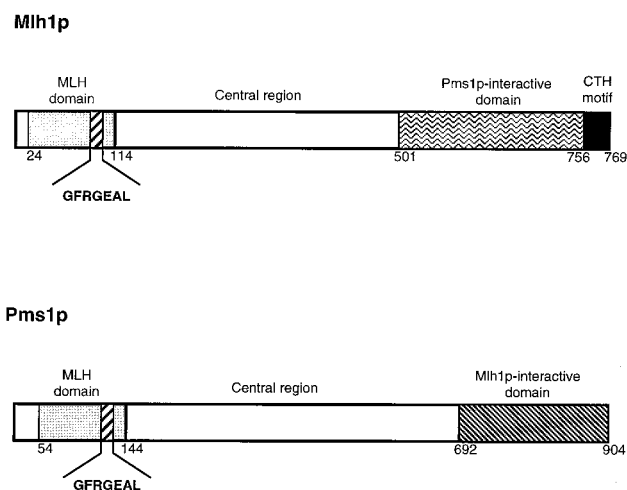


FIG. 6. Schematic structures of Mlh1p and Pms1p. The conserved amino-terminal MLH domain consists of 90 residues in each protein and encompasses the MutL box sequence GFRGEAL. The CTH motif in Mlh1p contains the final 13 amino acids that are identical between the yeast Mlh1 and the hMLH1 proteins.

	SUBDOMAIN 1		SUBDOMAIN 2		SUBDOMAIN 3
<i>S. cerevisiae</i> Pms1p	722 VDNKSDLFIVD QHAS DEKYNFETL (100)		RACR SS IMIG (20)		FWNC PHGRPTM 886
<i>S. cerevisiae</i> Mlh3p	513 IHNCP LLVLVDQ HACDERIRLEEL (131)		KACR SAV MFG (20)		PFEC AHGR PSM 709
Consensus sequence	VX N XX L XI V D Q H A X D E K XX X E L (100-131)		RACR SS IM X G (20)		FWNC X H G R P T M
	I L R		K AV		FE S

FIG. 7. Subdomains conserved between the Mlh1p-interactive domain of Pms1p [Pms1p(692–904)] and the carboxyl-terminal portion of Mlh3p (accession number Z73520). Bold letters correspond to identical amino acids. X, nonconserved residue. The number of residues between the different subdomains is indicated in parentheses.

of a direct mismatch repair activity for MutL proteins, a novel class of ATP binding and hydrolysis domains appears to be conserved among the B subunit of the type II topoisomerases, *E. coli* gyrase, and the MutL protein family (9). Both *E. coli* gyrase and the type II topoisomerase subunit B can bind an ATP analog (9, 24). The three putative ATP-binding motifs are present in the MLH domain of Mlh1p and Pms1p (9) (Fig. 3). Therefore, the Mlh1p-Pms1p heterodimer may cooperate with Msh proteins in providing the ATP binding and hydrolysis functions necessary for mismatch correction.

The dominant negative effect of overexpression of the MutL box mutants Mlh1p-F96A and Pms1p-F126A and the CTH motif deletion Mlh1p(1–761) may result from mutant proteins that form nonfunctional Mlh1p-Pms1p dimers that either fail to interact appropriately with other proteins or cannot carry out a biochemical function, e.g., ATP binding and hydrolysis. In contrast, the dominant negative effects of Mlh1p(1–265), Mlh1p-K619del, and Mlh1p(734–769), all of which are unable to bind Pms1p, are likely to occur through a Pms1p-independent mechanism. These dominant negative effects may result from competitive titration of other critical components, e.g., proteins of the repair complex. The dominant negative mutator effect of Mlh1p-K619del is analogous to the effect of an hMLH1 mutant, i.e., hmlh1-K618del, that appears to compromise DMR activity in normal cells of HNPCC patients (45). We stress that the dominant negative effects in the present study appear to require overexpression of the mutant proteins (Fig. 5). Therefore, in the case of the potential hMLH1 dominant negative mutation (45), we would predict that the mutant allele is expressed at a level higher than the level of expression of the wild-type allele. Supporting this argument is the recent observation that a human *PMS2* nonsense mutation, *hPMS2-134* (45), that appears to be a dominant negative germline mutation is expressed at a significantly higher level than the level of expression of the wild-type allele in cells from clinically affected patients (41a).

Recently, Aronshtam and Marinus (5) have reported the use of dominant negative mutations to identify functional domains of *E. coli* MutL protein. These dominant negative effects also required high-level expression of the mutant proteins. Most MutL dominant negative mutations were found to be located in the conserved amino-terminal portion of the MutL protein (5), a finding that supports our observations with yeast. Furthermore, multicopy plasmids containing the wild-type *mutS* or *mutH* gene could suppress the dominant negative mutations in the *mutL* gene encoding the carboxyl-terminal but not the amino-terminal part of the protein, suggesting that the two parts of the MutL protein might perform different functions (5). It will be of interest to ask whether overexpression of certain genes (e.g., *MSH2* and *MSH6*) can overcome the dominant negative effect of the *MLH1* and *PMS1* mutations.

Finally, recent work suggests that an early step in DMR in both yeast and human requires the replication processivity protein PCNA (54). In yeast, Pcnap was shown to interact with both Mlh1p and Msh2p, suggesting a linkage between the

Mlh1p and Mshp heterodimers. However, Mlh1p mutants with point mutations in the MutL box no longer interact with Pcnap (51a), although the Mlh1p-Pms1p interaction is preserved, suggesting that the MutL box of Mlh1p may be involved in the Mlh1p-Pcnap interaction and thus in the formation of a higher-order DMR complex. In summary, our results support a model in which one of the functions of the Mlh1p-Pms1p heterodimer is to recruit other components to the mismatch repair complex. Like Mlh1p-Pms1p interaction, the putative interaction of the Mlh1p-Pms1p heterodimer with other proteins is presumably necessary for the DMR function. The results of the domain mapping of Mlh1p and Pms1p presented here should aid in the identification of new components in the DMR process and in the evaluation of the functional and disease significance of mutations found in the human MutL homologs in cancer families.

ACKNOWLEDGMENTS

We thank Deborah Lycan, Andrew Buermeier, and Erica Shelley for valuable comments on the manuscript. We also thank Jeff Simon for construction of plasmid vectors pCoB-5006 and pJAS.

This work was supported by National Institutes of Health grant GM45413 and National Science Foundation grant MCB9314116 to R.M.L. and by a NSF Biosciences Related to the Environment postdoctoral fellowship to T.A.P.

REFERENCES

- Acharya, S., T. Wilson, S. Gradia, M. F. Kane, S. Guerrette, G. T. Marsischky, R. Kolodner, and R. Fishel. 1996. hMSH2 forms specific mismatch-binding complexes with hMSH3 and hMSH6. *Proc. Natl. Acad. Sci. USA* **93**:13629–13634.
- Alani, E. 1996. The *Saccharomyces cerevisiae* Msh2 and Msh6 proteins form a complex that specifically binds to duplex oligonucleotides containing mismatched DNA base pairs. *Mol. Cell. Biol.* **16**:5604–5615.
- Alani, E., R. A. G. Reenan, and R. Kolodner. 1994. Mismatch repair proteins directly affect gene conversion in *Saccharomyces cerevisiae* by regulating heteroduplex tract length. *Genetics* **137**:19–39.
- Alani, E., T. Sokolsky, B. Studamire, J. J. Miret, and R. S. Lahue. 1997. Genetic and biochemical analysis of Msh2p-Msh6p: role of ATP hydrolysis and Msh2p-Msh6p subunit interactions in mismatch base pair recognition. *Mol. Cell. Biol.* **17**:2436–2447.
- Aronshtam, A., and M. G. Marinus. 1996. Dominant negative mutator mutations in the *mutL* gene of *Escherichia coli*. *Nucleic Acids Res.* **24**:2498–2504.
- Baker, S. M., C. E. Bronner, L. Zhang, A. W. Plug, M. Robatzek, G. Warren, E. A. Elliott, J. Yu, T. Ashley, N. Arnheim, R. A. Flavell, and R. M. Liskay. 1995. Male mice defective in the DNA mismatch repair gene *PMS2* exhibit abnormal chromosome synapsis in meiosis. *Cell* **82**:309–319.
- Baker, S. M., A. W. Plug, T. A. Prolla, C. E. Bronner, A. C. Harris, X. Yao, D. M. Christie, C. Monell, N. Arnheim, A. Bradley, T. Ashley, and R. M. Liskay. 1996. Involvement of mouse Mlh1 in DNA mismatch repair and meiotic crossing over. *Nat. Genet.* **13**:336–342.
- Bartel, P., C. T. Chien, R. Strenglanz, and S. Fields. 1993. Elimination of false positives that arise in using the two-hybrid system. *BioTechniques* **14**:920–924.
- Bergerat, A., B. de Massy, D. Gabelle, P.-C. Varoutas, A. Nicolas, and P. Forterre. 1997. An atypical topoisomerase II from archaea with implications for meiotic recombination. *Nature (London)* **386**:414–417.
- Bishop, D. K., J. Andersen, and R. D. Kolodner. 1989. Specificity of mismatch repair following transformation of *Saccharomyces cerevisiae* with heteroduplex plasmid DNA. *Proc. Natl. Acad. Sci. USA* **86**:3713–3717.
- Bradford, M. 1976. A rapid and sensitive method for the quantitation of

- microgram quantities of protein using the principal of dye binding. *Anal. Biochem.* **72**:248–254.
12. Bronner, C. E., S. M. Baker, P. T. Morrison, G. Warren, L. G. Smith, M. Lescoe, M. Kane, C. Earabino, J. Lipford, A. Lindblom, P. Tannergard, R. J. Bollag, A. R. Godwin, D. C. Ward, M. Nordenskjold, R. Fishel, R. Kolodner, and R. M. Liskay. 1994. Mutation in the DNA mismatch repair gene homologue *hMLH1* is associated with hereditary non-polyposis colon cancer. *Nature (London)* **368**:258–261.
 13. Cunningham, B. C., and J. A. Wells. High-resolution epitope mapping of hGH-receptor interactions by alanine-scanning mutagenesis. *Science* **244**:1081–1085.
 14. de Wind, N., M. Dekker, A. Berns, M. Radman, and H. te Riele. 1995. Inactivation of the mouse *Msh2* gene results in mismatch repair deficiency, methylation tolerance, hyperrecombination, and predisposition to cancer. *Cell* **82**:321–330.
 15. Drummond, J. T., G.-M. Li, M. J. Longley, and P. Modrich. 1995. Mismatch recognition by an hMSH2-GTBP heterodimer and differential repair defects in tumor cells. *Science* **268**:1909–1912.
 16. Edelmann, W., P. E. Cohen, M. Kane, K. Lau, B. Morrow, S. Bennett, A. Umar, T. Kunkel, G. Cattoretti, R. Chaganti, J. W. Pollard, R. D. Kolodner, and R. Kucherlapati. 1996. Meiotic pachytene arrest in *MLH1*-deficient mice. *Cell* **85**:1125–1134.
 17. Field, J., J.-I. Nikawa, D. Broek, B. MacDonald, L. Rodgers, I. A. Wilson, R. A. Lerner, and M. Wigler. 1988. Purification of a *RAS*-responsive adenylyl cyclase complex from *Saccharomyces cerevisiae* by use of an epitope addition method. *Mol. Cell. Biol.* **8**:2159–2165.
 18. Fishel, R., M. K. Lescoe, M. R. Rao, N. G. Copeland, N. A. Jenkins, J. Garber, M. Kane, and R. Kolodner. 1994. The human mutator gene homolog *MSH2* and its association with hereditary nonpolyposis colon cancer. *Cell* **75**:1027–1038.
 19. Gietz, D., A. S. Jean, R. A. Woods, and R. H. Schiestl. 1992. Improved method for high efficiency transformation of intact yeast cells. *Nucleic Acids Res.* **20**:1425–1430.
 20. Grilley, M., K. M. Welsh, S. S. Su, and P. Modrich. 1989. Isolation and characterization of the *Escherichia coli* *mutL* gene product. *J. Biol. Chem.* **264**:1000–1004.
 21. Haber, L. T., and G. C. Walker. 1991. Altering the conserved nucleotide binding motif in the *Salmonella typhimurium* MutS mismatch repair protein affects both its ATPase and mismatch binding activities. *EMBO J.* **10**:2707–2715.
 22. Habraken, Y., P. Sung, L. Prakash, and S. Prakash. 1996. Binding of insertion/deletion DNA mismatches by the heterodimer of yeast mismatch repair proteins MSH2 and MSH3. *Curr. Biol.* **6**:1185–1187.
 23. Iaccarino, I., F. Palombo, J. Drummond, N. F. Totty, J. J. Hsuan, P. Modrich, and J. Jiricny. 1996. MSH6, a *Saccharomyces cerevisiae* protein that binds to mismatches as a heterodimer with MSH2. *Curr. Biol.* **6**:484–486.
 24. Jackson, A. P., and A. Maxwell. 1993. Identifying the catalytic residue of the ATPase reaction of DNA gyrase. *Proc. Natl. Acad. Sci. USA* **90**:11232–11236.
 25. Johnson, R. E., G. K. Kovvali, L. Prakash, and S. Prakash. 1996. Requirement of the yeast *MSH3* and *MSH6* genes for *MSH2* dependent genomic stability. *J. Biol. Chem.* **271**:7285–7288.
 26. Kolodner, R. 1996. Biochemistry and genetics of eukaryotic mismatch repair. *Genes Dev.* **10**:1433–1442.
 27. Kramer, B., W. Kramer, M. S. Williamson, and S. Fogel. 1989. Heteroduplex DNA correction in *Saccharomyces cerevisiae* is mismatch repair specific and requires functional *PMS1* genes. *Mol. Cell. Biol.* **9**:4432–4440.
 28. Kramer, W., B. Kramer, M. S. Williamson, and S. Fogel. 1989. Cloning and nucleotide sequence of DNA mismatch repair gene *PMS1* from *Saccharomyces cerevisiae*: homology of *PMS1* to prokaryotic MutL and HexB. *J. Bacteriol.* **171**:5339–5346.
 29. Leach, F. S., N. C. Nicolaides, N. Papadopoulos, B. Liu, J. Jen, R. Parsons, P. Peltomaki, P. Sistonen, L. A. Aaltonen, M. Nystrom-Lahti, X.-Y. Guan, J. Zhang, P. S. Meltzer, J.-W. Yu, F.-T. Kao, D. J. Chen, K. M. Cerosaletti, R. E. K. Fournier, S. Todd, T. Lewis, R. J. Leach, S. L. Naylor, J. Weissenbach, J.-P. Mecklin, H. Jarvinen, G. M. Petersen, S. R. Hamilton, J. Green, J. Jass, P. Watson, H. T. Lynch, J. M. Trent, A. de la Chapelle, K. W. Kinzler, and B. Vogelstein. 1993. Mutations of a mutS homolog in hereditary nonpolyposis colorectal cancer. *Cell* **75**:1215–1225.
 30. Li, G.-M., and P. Modrich. 1995. Restoration of mismatch repair to nuclear extracts of H6 colorectal tumor cells by a heterodimer of human MutL homologs. *Proc. Natl. Acad. Sci. USA* **92**:1950–1954.
 31. Lu, A. L., K. Welsh, S. Clark, S. S. Su, and P. Modrich. 1984. Repair of DNA base-pair mismatches in extracts of *Escherichia coli*. *Cold Spring Harbor Symp. Quant. Biol.* **49**:589–596.
 32. Luria, S. E., and M. Delbruck. 1943. Mutations of bacteria from virus sensitivity to virus resistance. *Genetics* **28**:491–511.
 33. Lynch, H. T., T. C. Smyrk, P. Watson, S. J. Lanspa, J. F. Lynch, P. M. Lynch, R. J. Cavalieri, and C. R. Boland. 1993. Genetics, natural history, tumor spectrum, and pathology of hereditary nonpolyposis colorectal cancer: an updated review. *Gastroenterology* **104**:1535–1549.
 34. Maniatis, T., E. F. Fritsch, and J. Sambrook. 1982. Molecular cloning: a laboratory manual. Cold Spring Harbor Laboratory, Cold Spring Harbor, N.Y.
 35. Mankovich, J. A., C. A. McIntyre, and G. C. Walker. 1989. Nucleotide sequence of the *Salmonella typhimurium* *mutL* gene required for mismatch repair: homology of MutL to HexB of *Streptococcus pneumoniae* and to PMS1 of the yeast *Saccharomyces cerevisiae*. *J. Bacteriol.* **171**:5325–5331.
 36. Marsischky, G. T., N. Filosi, M. F. Kane, and R. Kolodner. 1996. Redundancy of *Saccharomyces cerevisiae* *MSH3* and *MSH6* in *MSH2*-dependent mismatch repair. *Genes Dev.* **10**:407–420.
 37. Michael, A. I., D. H. Gelfand, J. J. Sninsky, and T. J. White. 1990. PCR protocols: a guide to method and applications. Academic Press, San Diego, Calif.
 38. Miller, J. H. 1972. Experiments in molecular genetics. Cold Spring Harbor Laboratory, Cold Spring Harbor, N.Y.
 39. Modrich, P. 1991. Mechanisms and biological effects of mismatch repair. *Annu. Rev. Genet.* **25**:229–253.
 40. Modrich, P., and R. Lahue. 1996. Mismatch repair in replication fidelity, genetic recombination, and cancer biology. *Annu. Rev. Biochem.* **65**:101–133.
 41. New, L., K. Liu, and G. F. Crouse. 1993. The yeast gene *MSH3* defines a new class of eukaryotic MutS homologues. *Mol. Gen. Genet.* **239**:97–108.
 - 41a. Nicolaides, N., R. Parsons, and B. Vogelstein. Personal communication.
 42. Nicolaides, N. C., N. Papadopoulos, B. Liu, Y. F. Wei, K. C. Carter, S. M. Ruben, C. A. Rosen, W. A. Haseltine, R. D. Fleischmann, C. M. Fraser, M. D. Adams, J. C. Venter, M. G. Dunlop, S. R. Hamilton, G. M. Peterson, A. de la Chapelle, B. Vogelstein, and K. W. Kinzler. 1994. Mutations of two *PMS* homologues in hereditary nonpolyposis colon cancer. *Nature (London)* **371**:75–80.
 43. Palombo, F., I. Iaccarino, E. Nakajima, M. Iejima, T. Shimada, and J. Jiricny. 1996. hMutS β , a heterodimer of hMSH2 and hMSH3, binds to insertion/deletion loops in DNA. *Curr. Biol.* **6**:1181–1184.
 44. Papadopoulos, N., N. C. Nicolaides, Y.-F. Wei, S. M. Ruben, K. C. Carter, C. A. Rosen, W. A. Haseltine, R. D. Fleischmann, C. M. Fraser, M. D. Adams, J. C. Venter, S. R. Hamilton, G. M. Petersen, P. Watson, H. T. Lynch, P. Peltomaki, J. P. Mecklin, A. de la Chapelle, K. W. Kinzler, and B. Vogelstein. 1994. Mutation of a *mutL* homolog in hereditary colon cancer. *Science* **263**:1625–1628.
 45. Parsons, R., G.-M. Li, M. Longley, P. Modrich, B. Liu, T. Berk, S. R. Hamilton, K. W. Kinzler, and B. Vogelstein. 1995. Mismatch repair deficiency in phenotypically normal human cells. *Science* **268**:738–740.
 46. Prolla, T. A., D. M. Christie, and R. M. Liskay. 1994. Dual requirement in yeast DNA mismatch repair for *MLH1* and *PMS1*, two homologs of the bacterial *mutL* gene. *Mol. Cell. Biol.* **14**:407–415.
 47. Prolla, T. A., Q. Pang, E. Alani, R. D. Kolodner, and R. M. Liskay. 1994. Interaction between the MSH2, MLH1 and PMS1 proteins during the initiation of DNA mismatch repair in yeast. *Science* **265**:1091–1093.
 48. Prudhomme, M., B. Martin, V. Mejean, and J.-P. Claverys. 1989. Nucleotide sequence of the *Streptococcus pneumoniae* *hexB* mismatch repair gene: homology of HexB to MutL of *Salmonella typhimurium* and to PMS1 of *Saccharomyces cerevisiae*. *J. Bacteriol.* **171**:5332–5338.
 49. Reitmaier, A. H., R. Schmits, A. Ewel, B. Bapat, M. Redston, A. Mitri, P. Waterhouse, H. W. Mittrucker, A. Wakeham, B. Liu, A. Thomason, A. Mitri, M. Redston, S. Gallinger, R. Bristol, R. Hills, M. Meuth, W. Ballhausen, R. Fishel, and T. Mak. 1995. MSH2 deficient mice are viable and susceptible to lymphoid tumours. *Nat. Genet.* **11**:64–70.
 50. Ross-Macdonald, P., and G. S. Roeder. 1994. Mutation of a meiosis-specific MutS homolog decreases crossing over but not mismatch correction. *Cell* **79**:1069–1080.
 51. Sancar, A., and J. E. Hearst. 1993. Molecular matchmakers. *Science* **259**:1415–1420.
 - 51a. Simon, J., and R. M. Liskay. Unpublished data.
 52. Thibodeau, S. N., G. Bren, and D. Schaid. 1993. Microsatellite instability in cancer of the proximal colon. *Science* **260**:816–819.
 53. Tyers, M., G. Tokiwa, R. Nash, and B. Futcher. 1992. The Cln3-Cdc28 kinase complex of *S. cerevisiae* is regulated by proteolysis and phosphorylation. *EMBO J.* **11**:1773–1784.
 54. Umar, A., A. B. Buermeier, J. A. Simon, D. C. Thomas, A. B. Clark, R. M. Liskay, and T. A. Kunkel. 1996. Requirement for PCNA in DNA mismatch repair at a step preceding DNA resynthesis. *Cell* **87**:65–73.
 55. Umar, A., and T. A. Kunkel. 1996. DNA-replication fidelity, mismatch repair and genome instability in cancer cells. *Eur. J. Biochem.* **238**:297–307.
 56. Vojtek, A. B., S. M. Hollenberg, and J. A. Cooper. 1993. Mammalian ras interacts directly with the serine/threonine kinase raf. *Cell* **74**:205–214.
 57. Wu, T.-H., and M. G. Marinus. 1994. Dominant negative mutator mutations in the *mutS* gene of *Escherichia coli*. *J. Bacteriol.* **176**:5393–5400.